Pergamon

Carbon, Vol. 32, No. 8, pp. 1499–1505, 1994

0008-6223/94 $6.00 + .00

0008-6223(94)00104-9

EFFECT OF CHEMISORBED OXYGEN ON THE ELECTROCHEMICAL BEHAVIOR OF GRAPHITE FIBERS

CHRISTINE A. FRYSZ
Wilson Greatbatch Ltd., 10,000 Wehrle Drive, Clarence, New York 14031, U.S.A.

and

XIAOPING SHUI and D. D. L. CHUNG
Composite Materials Research Laboratory, Furnas Hall,
State University of New York at Buffalo,
Buffalo, New York 14260-4400, U.S.A.

(*Received* 16 *May* 1994; *accepted in revised form* 11 *July* 1994)

Abstract—The effect of chemisorbed oxygen on the electrochemical behavior of radially structured graphite fibers (Amoco Thornel P100) was studied. The outer graphite skin was removed by heating in air, allowing the edge plane sites to be exposed and increasing the concentration of chemisorbed oxygen. Mass spectrometry, conducted while heating the oxidized fibers, detected primarily carbon monoxide, suggesting that the chemisorbed oxygen was in the form of phenol, carbonyl, and/or quinone functional groups. Cyclic voltammetry showed that the electron transfer rate and reversibility of the iron cyanide redox species increased, the voltammetric peak separation decreased, and the cathodic peak current density approached the anodic peak current density as the burn-off level increased from 0% to 17%. Moreover, a decrease in surface tension accompanied by an increase in wettability of the fiber by the electrolyte was observed upon burn-off by 17%. Subsequent reduction in hydrogen resulted in a large increase in surface tension, a decrease in the surface oxygen concentration, an increase in the oxygen-binding energy and a dramatic loss of electrochemical activity. The investigation demonstrates that the domination of edge sites produced by thermally removing the basal plane surface skin of the fibers resulted in the formation of oxygen-containing surface functional groups that reduced the fiber surface tension (increasing wettability), thereby improving the electron transfer rate and electrochemical reversibility.

Key Words—Oxygen, graphite fibers, carbon fibers, electrochemical, chemisorption, voltammetry.

1. INTRODUCTION

Carbon and graphite fibers were introduced into the commercial market in the mid 1960s. They are commonly used as structural reinforcing agents because they are light in weight and can be prepared to display high strength and modulus. Recently, however, researchers have explored their use in electrodes, particularly microelectrodes, for electroanalytical and bioanalytical studies[1,2]. For these applications, electrochemical behavior of the fibers is important.

The electrochemical response of carbon and graphite materials can be enhanced by oxidation, either electrochemically, chemically, or thermally. The concentration of surface oxides produced is associated with the edge-to-basal-surface-area ratio. Studies using highly oriented pyrolytic graphite (HOPG) have compared the electrochemical performance of the basal and edge surfaces for $Fe(CN)_6^{-3/-4}$[3]. Results show that the electrochemical behavior of the edge surface is superior to that of the basal surface; the basal surface is extremely unreactive. The electron transfer rate and the capacitance of the edge surface are significantly higher. Also, the $Fe(CN)_6^{-3/-4}$ reaction on the edge surface is more reversible than on the basal surface, with the anodic-to-cathodic peak potential difference (ΔE) at a scan rate of 200 mV/s approximately 70 mV. The activity coefficient (k) was determined to be at least 10^5 times that obtained for the basal surface. It is expected, therefore, that the electrochemical behavior of carbon fibers will be dependent upon the proportions of edge and basal surface areas. Studies conducted with carbon fibers displaying 'random' and 'onion' type microstructures show that the electrochemical performance of the cylindrical surfaces is very poor in comparison to that of the tip[4]. This observation is consistent with the mainly basal plane character usually present on the surface of these fibers.

Carbon and graphite surfaces, being reactive because of the presence of unsatisfied valences, readily chemisorb oxygen-containing molecules[5]. The type and concentration of the functional groups chemisorbed influence the material's electrochemical behavior. The objective of this paper is to investigate the electrochemical behavior of radially structured graphite fibers, namely, Amoco's Thornel P100, as a function of thermal oxidation. These fibers are unsized, high-modulus, mesophase-pitch-based graphite fibers.

2. EXPERIMENTAL

Oxygen chemisorption was effected by thermal treatment in air. The graphite fibers were isothermally

heated to 600°C, then held at this temperature until various levels of burn-off were achieved. Burn-off levels were determined via sample weight loss. The effects of the thermal treatment were evaluated using various analytical techniques. Surface elements were analyzed using electron spectroscopy for chemical analysis (ESCA), a high-vacuum surface science technique. To measure the oxygen chemisorption of the fibers, desorption was conducted in a thermogravimetric analyzer (Perkin-Elmer TGA7) after oxidation burn-off; the oxidized fibers were heated in purified helium to 1450°C at a rate of 20°C per minute, and the weight loss was recorded as a function of temperature. In addition, the evolved gas during desorption was analyzed by mass spectroscopy during heating and was shown to be predominantly CO (rather than CO_2).

The specific oxygen adsorption area (SOAA) in m^2/g was calculated using the equation

$$\text{SOAA} = \frac{(\text{Weight loss})(6.023 \times 10^{23})(8.3 \times 10^{-20}\ \text{m}^2)}{28\ (\text{Original sample weight})}, \quad (1)$$

where 28 is the molecular weight of carbon monoxide in atomic mass units, 8.3×10^{-20} is the area occupied by one atom of oxygen in m^2, and 6.023×10^{23} is Avogadro's number. It was assumed that only monolayer oxygen existed on the surface and that each oxygen atom occupied 8.3 square Ångstroms[6].

The microstructure and surface condition of the oxidized fibers were characterized using a scanning electron microscope (SEM). Electrochemical performance was assessed by cyclic voltammetry (CV). The test solution in CV comprised 6 mM potassium ferricyanide (or potassium hexacyanoferrite (III) in IUPAC nomenclature) [$K_3Fe(CN)_6$] as the electroactive species in 1 M potassium nitrate [KNO_3] in water as the supporting electrolyte. The three-electrode system used included a saturated calomel reference electrode, a platinum wire auxiliary electrode and a bundle of the graphite fibers under study as the working electrode. Voltammograms began sufficiently negative of the ferricyanide potential to allow reduction of the electroactive species in solution to ferrocyanide. Cycling then began with the oxidation half cycle at scan rates of 20, 50, 75, 100, 125, 150, 175, and 200 mV/s.

The wettability of the oxidized fibers was evaluated using the static Wilhelmy method[7]. The set-up for this procedure is illustrated in Fig. 1. A single graphite fiber was suspended from a fixture. A beaker with the wetting electrolyte, in this case the same solution as used for CV, was raised toward the suspended fiber until the fiber tip just touched the solution surface. The change in fiber weight due to the fluid was recorded using a Mettler Analytical Balance with a sensitivity of 0.0001 g. The contact angle, ϕ, of the liquid with the fiber was measured using a protractor. The fiber tip was magnified and then photographed to facilitate the measurement. The surface tension was obtained by the equation

$$\gamma = \frac{\Delta W}{P \cos \phi}, \quad (2)$$

where

γ = surface tension,
ΔW = weight change or force exerted by the fluid,
P = circumference of the fiber, and
ϕ = contact angle.

3. RESULTS AND DISCUSSION

Structurally, the P100 graphite fiber exhibits a 'bicycle wheel' or radial morphology encased in a 'skin' of graphite. By 3 hours of oxidation in air at 600°C, a 17% burn-off was achieved, resulting in complete removal of the 'skin.' An SEM view of the as-received fiber tip with the graphite 'skin' still in place and that of the tip with its skin thereby removed are shown in Fig. 2(a) and 2(b), respectively. For clarification, corresponding schematics are shown in Fig. 3(a) and 3(b), respectively. The basal plane is represented by the radial lines shown internal to the fiber, whereas the basal plane of the 'skin' is parallel to the cylindrical fiber surface.

The effects of burn-off on the surface morphology of the fiber are shown in Fig. 4. The as-received condition is depicted in Fig. 4(a). After 7% burn-off [Fig. 4(b)], the removal of the outer graphite 'skin' begins, resulting in a roughened appearance of the fiber surface. As the level of oxidation increases, yielding a 17% burn-off, the 'skin' appears to be fully removed, with 'holes' visible on the fiber surface [Fig. 4(c)]. After burn-off to 22% [Fig. 4(d)], the 'holes' appear to penetrate more deeply into the fiber interior. Schematically, these observations are shown in Fig. 5. The cross-section of the as-received fiber is shown in Fig. 5(a). When a 7% burn-off takes place, surface roughening is conceptualized as the thinning of the 'skin' with areas of total depletion, or 'holes,'

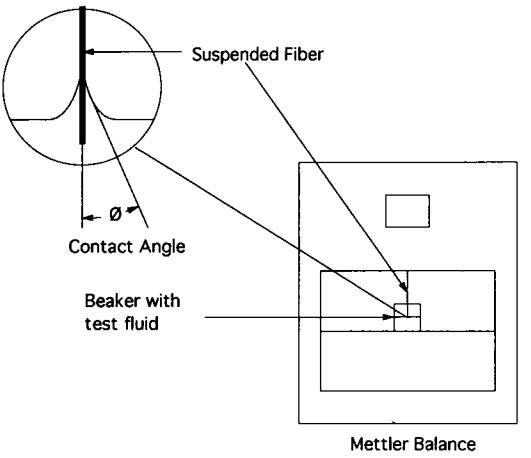

Fig. 1. Setup for the static Wilhelmy method for the determination of surface energy.

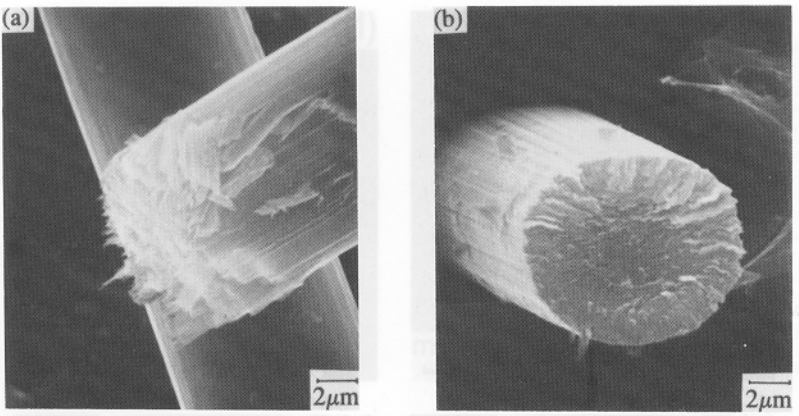

Fig. 2. SEM view of (a) the as-received graphite fiber and (b) the tip of the fiber after 17% burn-off.

randomly dispersed over the fiber surface [Fig. 5(b)]. The 'holes' are most likely fully exposed edge plane and defect sites. Complete removal of the 'skin' (the external basal plane) with minor penetration into the fiber interior occurs at 17% burn-off. Electrochemical activity then is predominantly associated with the newly exposed edge plane and defect sites. Further oxidation to a 22% burn-off has a negligible effect on the number of edge plane and defect sites on the fiber surface. However, deeper penetration into the fiber interior results in increased basal plane exposure.

Oxygen chemisorption is known to occur predominantly on the edge rather than on the basal sites of graphitic materials[8,9]. The active area, in general, is directly associated with the concentration of edge sites available for chemisorption. For the P100 fibers, the SOAA values are shown in Table 1. Under the assumption that oxygen was chemisorbed as monolayer oxygen, the molecular weight of carbon monoxide was used to calculate SOAA. As expected, SOAA increases with increasing burn-off. The largest SOAA increase occurs between burn-off levels of 17% and 22%. From Table 1, it can be seen that the desorption onset temperature remains essentially the same from 0% to 17% burn-off. Between 17% and 22% burn-off, a significant decrease in desorption onset temperature occurs. This is shown graphically by the thermogravimetric data in Fig. 6. The SEM and desorption results indicate that, as burn-off increases from 17% to 22%, chemisorption occurs on the edge and defect sites exposed as the basal surface 'skin' is removed, and adsorption occurs at the gaps developed between the layers of the now-exposed basal plane. Bonding energies of the adsorbed species of the basal plane are most likely weaker than at the chemisorbed sites of the edge plane, yielding a lower desorption onset temperature at 22% burn-off (Table 1).

The oxides believed to be present on carbon and graphite surfaces include phenols, carbonyls, carboxyls, quinones, and lactones[10]. Schematics of these groups are shown in Fig. 7. The functional groups expected to desorb carbon monoxide include phenols, carbonyls, and quinones[10]. Mass spectroscopy was conducted during the desorption test on the 17% burn-off sample. Carbon monoxide was primarily detected, with a negligible amount of carbon dioxide. It may therefore be concluded that, of the possible functional groups on the surface of the fiber, phenols, carbonyls, and/or quinones are likely.

Cyclic voltammetry (CV) results are displayed in Fig. 8(a) through 8(d). The electrochemical response after 7% burn-off [Fig. 8(b)] was improved over that of the as-received P100 fiber [Fig. 8(a)]. As the level of oxidation increases, the electron transfer rate (shown by the small variation of the peak potential with the scan rate) and the reaction reversibility (shown by the relatively small difference between the oxidation

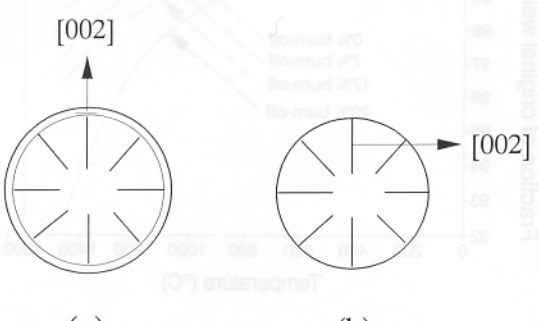

Fig. 3. Schematic of (a) the tip of the as-received graphite fiber and (b) the tip of the fiber after 17% burn-off.

Table 1. Chemisorption results (600°C in air)

Time at temperature (hours)	0	1.5	3.5	5.0
Prior burn-off (%)	0	7	17	22
SOAA (m^2/g)	0.95	4.28	6.98	19.8
Desorption onset temperature (°C)	704	709	707	630

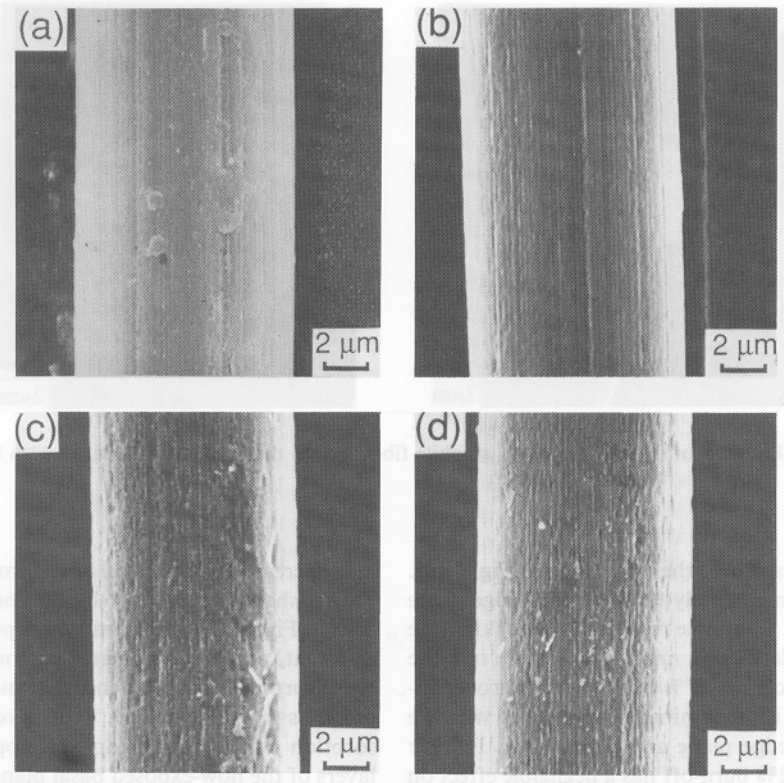

Fig. 4. SEM view of the side of (a) the as-received graphite fiber, (b) the 7% burn-off fiber, (c) the 17% burn-off fiber, and (d) the 22% burn-off fiber.

and reduction peak potentials) continue to improve [Fig. 8(c)]. No further advantage is realized at 22% burn-off [Fig. 8(d)] compared to 17% burn-off [Fig. 8(c)]. Data obtained from the CV curves (Table 2) indicate a decrease in both the voltammetry peak separation (ΔE) and in the anodic-to-cathodic peak current density ratio (I_a/I_c) from 0 to 17% burn-off, but from 17% to 22% burn-off, both the peak separation and the peak current density ratio increase slightly. The slight degradation in the electrochemical performance as oxidation progresses to a 22% weight loss is attributed to the reduction of the amount of edge sites and exposure of the basal planes interior to the fiber.

Four possible scenarios to explain the observed effect of oxidation on the electrochemical response are

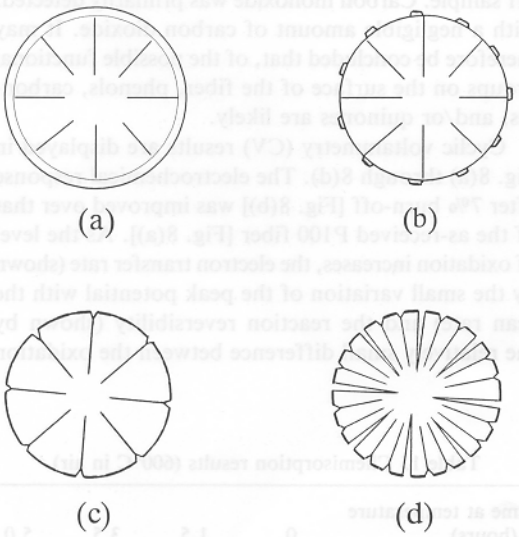

Fig. 5. Schematics of (a) the as-received graphite fiber, (b) the 7% burn-off fiber, (c) the 17% burn-off fiber, and (d) the 22% burn-off fiber.

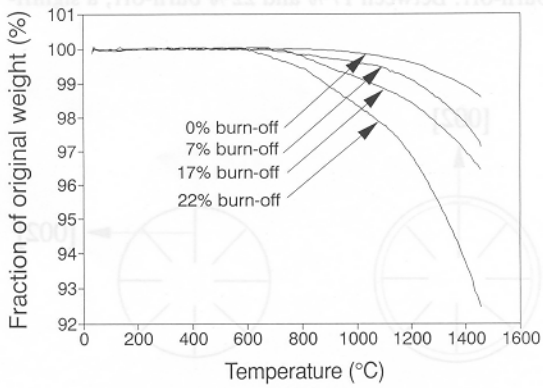

Fig. 6. Fraction of original weight before heating vs temperature during heating of fibers that had previously undergone various levels of burn-off.

Table 2. Cyclic voltammetry results (200 mV/s scan rate)

	As-received	7% burn-off	17% burn-off	22% burn-off
Anodic peak current density, I_a (mA/cm^2)	82	445	517	575
Cathodic peak current density, I_c (mA/cm^2)	451	866	614	724
I_a/I_c	5.5	1.9	1.2	1.3
Peak separation, ΔE (mV)	364	354	188	216

proposed. As schematically shown in Fig. 9, scenario 1 implies that the improvement in electrochemical behavior is due solely to the increased exposure of edge plane and defect sites. From scenario 2, the increase in edge plane and defect sites results in an increase in the amount of chemisorbed oxygen on the surface. The increase in the amount of chemisorbed oxygen may either improve the electrochemical performance directly (scenario 2), or result in scenario 3, whereby the increase in the amount of chemisorbed oxygen first induces a reduction in the fiber surface tension in the electrolyte, and then results in improved electrochemical activity. In scenario 4, the increase in edge plane and defect sites results in a reduced fiber surface tension, which then yields an improvement in the electrochemical response. To help distinguish among some of these scenarios, the surface tension of the fibers in the electrolyte (related to the wettability of the fibers by the electrolyte) was measured.

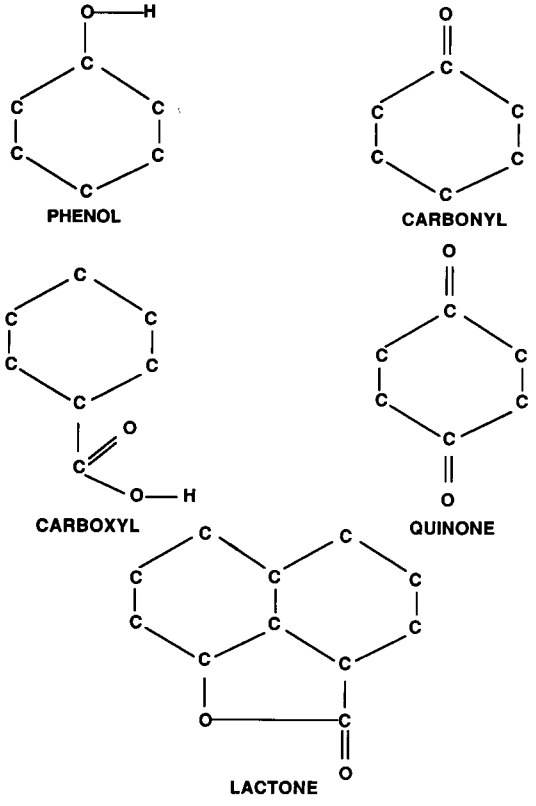

Fig. 7. Various functional groups on carbon.

The wettability of graphite had been studied by Dawe and Stevens[11]. It was demonstrated that graphite wettability increases as a function of oxidation. It was also found that wettability continues to increase with increasing heat-treating temperature up to 430°C. The possibility of a reduction in the surface tension of the P100 fibers was therefore examined. Using the static Wilhelmy method for determining the surface tension, the fiber weight and contact angle were measured. The results are summarized in Table 3. As expected, burn-off to 17% caused a decrease in the surface tension. Subsequent reduction in a 20:80 hydrogen:nitrogen atmosphere at 500°C for a duration of 2 hours resulted in a dramatic increase in the surface tension. ESCA was conducted to assess the oxygen content on the fiber surface before and after reduction. These results are summarized in Table 4. Note that reduction by hydrogen yielded an increase in the fiber surface carbon atom fraction, while the oxygen atom fraction decreased. Even though a substantial amount of oxygen remains on the surface after reduction, the increase in binding energy, although small, implies that the remaining oxygen is more tightly bonded, which should result in degradation in the electrochemical activity. CV conducted on the reduced sample is shown in Fig. 10. As expected, the resulting voltammogram demonstrates a dramatic degradation in the electrochemical response compared to that before reduction [Fig. 8(a)]. The conclusion, therefore, is that a high surface oxygen concentration (Table 4) is associated with a low surface tension (Table 3). The lowered surface tension means increased wettability. The increased wettability allows improved electrochemical response. Hydrogen

Table 3. Surface tension of carbon fibers in the electrolyte 6 mM $K_3Fe(CN)_6$

Sample	Surface tension (dynes/cm)
As-received	59 ± 5
17% burn-off	41 ± 5
17% burn-off and then reduced	214 ± 10

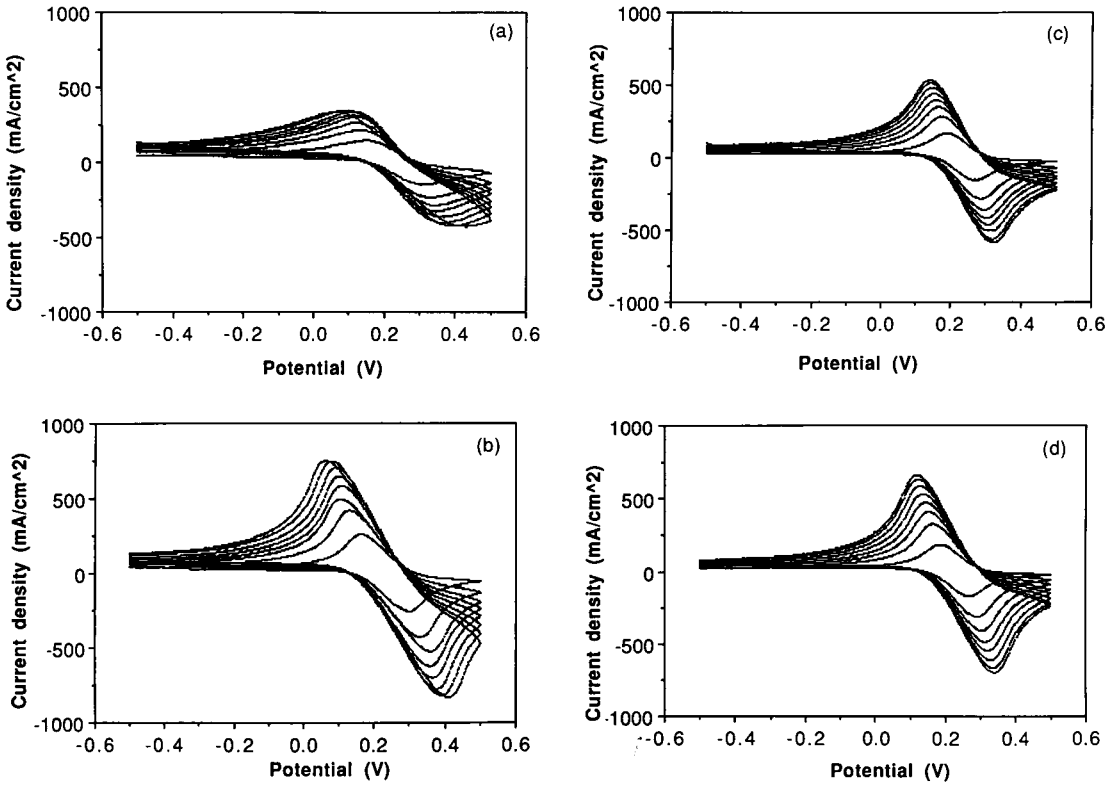

Fig. 8. Cyclic voltammogram of (a) the as-received graphite fiber, (b) the 7% burn-off fiber, (c) the 17% burn-off fiber, and (d) the 22% burn-off fiber. The different curves were obtained at different potential scan rates. The higher the scan rate, the higher the magnitude of the peak current density.

reduction results in a change in the graphite fiber surface functional group. As mentioned earlier, the functional groups suspected upon oxidation included phenols, carbonyls, and quinones, due to the fact that mass spectroscopy evolved predominantly carbon monoxide gas. The subsequent reduction then would result in either an increase in the number of phenol groups present as a result of hydrogen reaction with the existent carbonyl groups, or the formation of hydroquinones. Whichever transition occurred, the electrochemical activity was dramatically affected. Thus, scenarios 1 and 4 are eliminated from consideration.

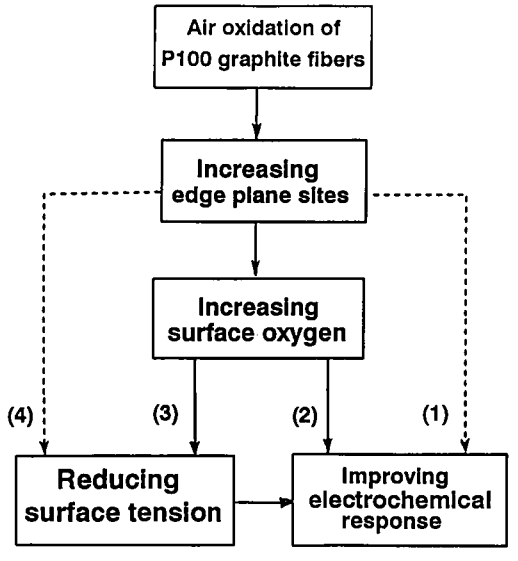

Fig. 9. Various scenarios to explain the observed effect of oxidation on the electrochemical response. Scenarios 2 and 3 are supported by this work, but not scenarios 1 and 4.

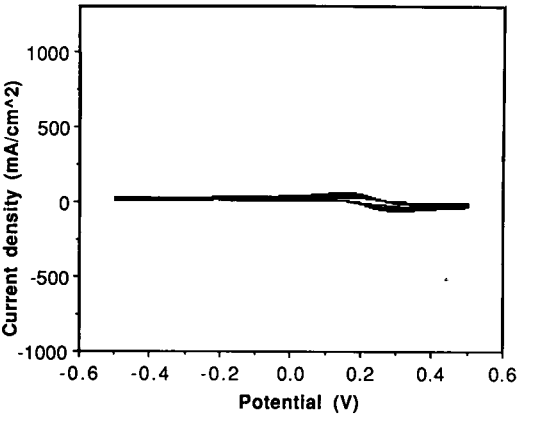

Fig. 10. Cyclic voltammogram after hydrogen reduction of the 17% burn-off fiber.

Table 4. ESCA results of fibers that had been heated in air to 17% burn-off and those that had been reduced after 17% burn-off

	17% burn-off sample		17% burn-off & reduced sample	
Element	Binding energy (eV)	At. %	Binding energy (eV)	At. %
C 1s	283.8	93.5	283.8	96.2
O 1s	531.3	6.5	531.7	3.8

4. CONCLUSIONS

The investigation conducted using Thornel P100 graphite fibers exhibiting a radial microstructure shows that removal of the graphite 'skin' via thermal treatment in air results in an increase in fiber surface edge and defect sites. These sites allow increased levels of oxygen chemisorption. The increase in oxygen concentration, shown to be a function of the level of burn-off as well as the microstructure of the fiber, resulted in increasing improvement in electrochemical activity. The enhancement of the electrochemical activity, evidenced by an increase in electron transfer rate and improved reversibility, is due to a decrease in the fiber surface tension which, in turn, increases the fiber wettability by the electrolyte. Although substantial oxygen remained on the fiber surface after hydrogen reduction, the change in the fiber surface functional group resulted in extremely depressed electrochemical activity. For electrode applications, then, the radially structured graphite fiber may provide advantages over random or onion-type fibers. They offer the ability to systematically remove basal surface character so that the edge sites dominate. The domination of edge sites allows sites for oxidation, which in turn allows formation of functional groups conducive to enhanced electrochemical activity.

Acknowledgements—This work was supported in part by the New York State Energy Research and Development Authority.

REFERENCES

1. R. M. Wightman and D. O. Wipf, *Electroanal. Chem.* **15**, 267 (1989).
2. M. Fleischmann, S. Pons, D. R. Rolison, and P. P. Schmidt, *Ultramicroelectrodes*, Datatech Systems, Inc. Science Publishers, Morgantown, NC (1987).
3. R. L. McCreery, *Electroanal. Chem.* **17**, 305 (1991).
4. J. Feng, M. Brazell, K. Renner, R. Kasser, and R. N. Adams, *Anal. Chem.* **59**, 1866 (1987).
5. R. L. McCreery, *Electroanal. Chem.* **17**, 258 (1991).
6. N. R. Laine, F. J. Vastola, and P. L. Walker, Jr., *J. Phys. Chem.* **67**, 2030 (1963).
7. Masahito Tagawa, N. Ohmae, M. Umeno, A. Yasukawa, K. Gotoh, and Mieko Tagawa, *J. Appl. Phys.* **30**, 2134 (1991).
8. R. O. Grisdale, *J. Appl. Phys.* **24**, 1288 (1953).
9. G. R. Hennig, *Proceedings of the Fifth Conference on Carbon*, Vol. 1, Pergamon Press, New York (1962), p. 143.
10. K. Kinoshita, *Carbon*, John Wiley and Sons, New York (1988), p. 87.
11. H. J. Dawe and R. F. Stevens, *Proceedings of the Fourth Conference on Carbon*, Pergamon Press, New York (1960), p. 17.